Advanced Powder Technology 35 (2024) 104513

Contents lists available at ScienceDirect

Advanced Powder Technology

journal homepage: www.elsevier.com/locate/apt

Multi-component mixing and demixing model for predictive finite element modelling of pharmaceutical powder compaction

Dingeman L.H. van der Haven [a], Maria Mikoroni [b], Andrew Megarry [c], Ioannis S. Fragkopoulos [b,*], James A. Elliott [a,*]

[a] Department of Materials Science & Metallurgy, University of Cambridge, 27 Charles Babbage Road, Cambridge CB3 0FS, United Kingdom
[b] Oral Drug Product Process Development, Novo Nordisk A/S, Måløv, Denmark
[c] Oral Formulation Research, Novo Nordisk A/S, Måløv, Denmark

ARTICLE INFO

Article history:
Received 31 January 2024
Received in revised form 23 April 2024
Accepted 4 June 2024

2020 MSC:
74C15
74E30
74L99
74S05

Keywords:
Powder compaction
Mixing
Formulation
Demixing
Unmixing

ABSTRACT

A set of numerical methods is described that allows predictive finite element method (FEM) simulations of the compaction of multi-component pharmaceutical powder formulations across the entire range of compositions. An automated parametrisation procedure was used to extract density-dependent Drucker-Prager Cap (dDPC) model parameters from experimental data. Subsequently, these parameters were interpolated (mixed) or extrapolated (demixed) to predict dDPC model parameters of unseen powder formulations. Pure, binary, and ternary formulations of micro-crystalline cellulose (MCC, plastic), dibasic calcium phosphate dihydrate (DCPD, brittle), and pre-gelatinised starch (STA, elastic) powders were used to validate the parametrisation and mixing/demixing methodologies. FEM simulations were capable of reproducing compaction curves with errors only marginally greater than the experimental variability. Using only pure component data, FEM simulations with mixing rules were capable of predicting the compaction curves of mixtures as well as their shear stress distributions. Moreover, with data of only two or three powder formulations, a new demixing methodology was able to predict the behaviour of the constituent powders. The combination of these methodologies provides a powerful tool to rapidly explore powder formulations anywhere within the composition phase diagram, providing compaction curves but also stress profiles that are essential to early-stage formulation process development and tooling design.

1. Introduction

The formation of mechanically stable tablets with suitable densities from cohesive powders is a critical process in the manufacture of many different products, such as powdered metals, foods, detergents, and pharmaceuticals. For instance in the pharmaceutical industry, such tablets are commonly made by direct compression of dry powders, which constitute a type of material known as granular matter. Direct compression is particularly interesting because it aligns with the current trend towards continuous manufacturing by enabling continuous processing. Despite the ubiquity of granular materials, our present-day understanding of them lags behind when compared to that of more classical types of matter such as gasses, liquids, and bulk solids for which most properties can be calculated as a function of their thermodynamic state. The complex interplay of numerous physical phenomena such as friction, cohesion, particle geometry, elasticity, plasticity, viscoelasticity, and viscoplasticity make it extremely challenging to discover predictive analytical theories. Even for the theories that have been discovered, such as Edwards statistical mechanics, the scope of their predictions remains heavily limited and many open problems still persist [1–3]. Combined with the exponential increase in computational power over the last decades, numerical methods have become the most popular approach for the predictive modelling of granular material.

Generally, numerical methods can be divided into one of three categories: discrete, continuum, or statistical. Discrete models, such as the discrete element method (DEM), explicitly consider each individual particle and are therefore expected to be the most predictive when experimental data are limited, but also suffer from a high com-

* Corresponding authors.
E-mail addresses: ifra@novonordisk.com (I.S. Fragkopoulos), jae1001@cam.ac.uk (J.A. Elliott).

https://doi.org/10.1016/j.apt.2024.104513

putational cost. Conversely, statistical methods are usually the least predictive as they require large quantities of experimental data, and extrapolations quickly become unreliable, but are computationally economic. The middle ground is filled by continuum methods, such as the finite element method (FEM), where the full material is divided into smaller elements, each of which behaves as a small piece of bulk material at an intermediate computational cost. FEM thus offers a good compromise between experimental data requirements, predictive capability, and computational cost. As a result, FEM has become one of the most popular methods for modelling powder compaction, and numerous studies have used FEM to study the effects of friction [4], punch geometry [5], elasticity [6], viscoelasticity [7], and even temperature [8] on tablets made by direct compression. Potential defects that are detrimental to tablet quality can thus be identified and the production processes can be adjusted to avoid such defects. This not only justifies the merit of FEM from an academic perspective, but also highlights its practical use by accelerating process development and solving tabletting problems before they lead to the delay of clinical trials. A recent review by Partheniadis et al. provides an excellent summary of the use of FEM for pharmaceutical tabletting applications [9].

FEM heavily relies on an accurate constitutive model and the proper parametrisation thereof. A popular choice is the density-dependent Drucker-Prager cap (dDPC) constitutive model, which is used in most of the studies using FEM to model tabletting [9]. A large part of this preference is due to the relatively modest requirements for experimental data; uniaxial compression experiments, powder compaction, and tablet crushing are sufficient for its parametrisation. Nonetheless, FEM with the dDPC model has clear limitations. Aside from the experimental data required, carrying out the parametrisation, i.e. transforming the experimental data into dDPC model parameters, requires significant effort. Parametrisations are typically done *ad hoc* for every formulation, resulting in a considerable time cost for each new powder to be simulated. Therefore, even models that have been proven to be predictive require a time investment on at least three fronts: 1) experimentation, 2) parametrisation, and 3) computation. Moreover, some of the required material, especially novel active pharmaceutical ingredients (APIs), may be scarce. Time and material investments can be manageable for a few powder mixtures, but these investments quickly become unmanageable for a larger numbers of formulations. Both time and materials are thus constraining factors in industry settings where a high throughput of different powder formulations is often required to obtain tablets of satisfactory quality.

Recently, van der Haven et al. reported an automated procedure for dDPC model parametrisation from experimental data, significantly reducing the time investment required for parametrisation [10]. However, time and material problems persist on the front of experimentation as each new formulation does still require new experimental data. The root of this problem lies in the fact that the number of possible powder formulations within the design space grows exponentially with the number of unique powders used. Therefore, even a formulation with only a few unique components might already be challenging to optimise with current methods. The aim of the current work is to minimise the experimental investment required for FEM formulation studies by validating and extending previously reported mixing methodologies.

The aforementioned obstacle in formulation and mixture optimisation is well-known and, in its general form, is a consequence of what is known colloquially as the curse of dimensionality. The general premise of any solution to the formulation problem is that, given a sufficient number of formulations with known properties, the properties of unseen formulations can be estimated. Several authors have pursued purely statistical models to address this challenge [11–14]. However, although useful, the lack of physicality in statistical models limits the insight they can provide and often requires large quantities of input data to fit them well. By far the most popular approach is to use physically-inspired mixing rules, particularly rules that use the volume fractions of the component powders. Mixing rules have already been used to successfully estimate tensile strengths [15–18], compressibility [19–22], powder flowability [23,24], critical drug loadings [25], tablet hardness [26], properties of individual components [27,28], and the effect of lubrication on porosity and tensile strength [29,30]. The utility of these models would be, for example, in predicting which areas of design space pharmaceutical tablets would meet certain minimum tensile strength criteria [31,32].

Nonetheless, a much higher degree of detail than just tensile strength provided by simple mixing rules is needed, such as a stress profile, to assure that a new formulation has a high chance of success in production settings. All of the aforementioned mixing studies only consider a single tablet geometry, often flat-faced tablets, whilst tablet shape and size are important design parameters, and generalising their results for other geometries is non-trivial. Moreover, even if such a generalisation were possible, the mixing rules provide no insight into common tabletting defects such as chipping, capping, and lamination [33–36]. These shortcomings again illustrate why, despite its simplicity, conventional Heckel analysis is usually insufficient. On the contrary, FEM simulations are capable of assessing the effects of tablet geometry and tooling friction, providing stress and density profiles that can be used to identify potential defects [4,5,33,34,37]. FEM thereby provides critical information to the tablet-design process that cannot be provided by simple mixing rules, but ultimately suffers from the same curse of dimensionality.

In a previous publication, the current authors proposed to combine FEM simulations with mixing rules, applying mixing rules directly to dDPC model parameters [10]. Using only experimental data of the pure constituent powders, we were able to carry out accurate FEM simulations of all mixtures. However, the study was limited in two main ways. First, only two materials and their binary mixtures were tested, leaving open the question of whether the framework remains valid for multi-component mixtures. Second, the previous method does not take into account the real possibility that some powders simply cannot be compacted in their pure form and is thereby limited to well-tabletable powders. The mixing rules were designed to be used on the dDPC model parameters of pure powders. However, not all pure powders allow the determination of their dDPC model parameters because some create tablets that immediately fall apart after ejection while tensile strength testing is required. An alternative must be found if one wants to predict the properties of mixtures containing one of these non-tabletable powders. In fact, this is a neglected problem within pharmaceutical powder formulation as there appears to be only one study, by Jolliffe et al., that addresses the determination of parameters of non-tabletable powders [28].

This work is thus a natural continuation of our previous study [10] and aims to expand the validity and applicability of the mixing method by validating mixing rules for ternary mixtures, including an additional 7 powder formulations, giving a total of 12 unique powder formulations. We also show that the updated mixing methodology can be used to dilute existing mixtures, allowing us to predict the properties of various formulations regardless of whether it contains a poorly or non-tabletable powder. Moreover, we propose a method to deconvolute powder formulations such that the properties, or dDPC model parameters, of any powder can determined using only mixtures, including those powders that are poorly tabletable. These developments allow accurate FEM simulations, usable for the improvement of the tablet-design process, for truly any mixture or formulation using minimal experimental data.

2. Experimental methods

2.1. Materials

The powders used in this study are micro-crystalline cellulose (MCC, Avicel PH200®), dibasic calcium phosphate dihydrate (DCPD, Emcompress premium®), and partially pregelatinized starch (Starch, SEPISTAB™ ST 200). The median particle diameters by volume, or D_v50 values, were 199, 212, and 192 μm, respectively. Aside from the 3 pure powders, this study considers 5 binary and 4 ternary mixtures, giving a total of 12 powder formulations. The compositions of all powder mixtures can be seen in Fig. 1, 2, 3, 4a, 6a, and 7a.

2.2. Data acquisition

All powder compaction experiments used the Medelpharm STYL'One Evolution press (Medelpharm, Beynost, France). The press was equipped with an external lubrication device (Medelpharm lubrication pack), a 80 kN load cell, circular flat-faced punches (11.28 mm), and an instrumented die. Punch deformation was determined and accounted for using the Analis software (Medelpharm, Beynost, France). Force sensors were dual-scale piezoelectric with an accuracy of 1 N, and displacement sensors had an accuracy of 1 μm. After external lubrication with magnesium stearate, the powder was filled into the die using a force feeder and compacted using a uniaxial, double-ended compaction, V-shape profile with a 0.2 mm s^{-1} punch speed (compression speed of 0.4 mm s^{-1}). Punches were centred around the radial pressure sensor in the die-wall. In the case of uniaxial compaction and axial symmetry on the z axis, the stresses in the tablet can be described using the hydrostatic stress

$$p = \frac{1}{3}(\sigma_z + 2\sigma_r) \tag{1}$$

and the von Mises equivalent stress

$$q = |\sigma_z - \sigma_r| \tag{2}$$

with σ_z the axial stress and σ_r the radial stress. For each formulation, tablets of 5 to 7 different densities were made with 10 to 12 replicates per density. The range of tablet densities was maximised by starting at the lowest density for which an intact cohesive tablet forms and ending at the highest density that still stays within the force limits of the compaction equipment. In total, this resulted in 73 unique tablets and 816 compactions.

Radial and axial fracture stresses were determined, each using three of the aforementioned replicates. Tablets were crushed using a Texture Analyser TA.XT.plusC (Stable Micro Systems, Surrey, United Kingdom) with a 50 kg load cell. For the tablets whose fracture stress surpassed the capabilities of the 50 kg load cell, the aforementioned STYL'One Evolution press was used to crush the tablets instead. The fracture stresses were calculated as

$$\sigma_r^f(\rho) = \frac{2F_{r,max}}{\pi D t} \tag{3}$$

for the radial direction and

$$\sigma_z^f(\rho) = \frac{4F_{z,max}}{\pi D^2} \tag{4}$$

for the axial direction, where D and t are respectively the tablet diameters and thickness, and $F_{r,max}$ and $F_{z,max}$ are the respective radial and axial maximum compression forces. Hereafter, Mohr–Coulomb theory can be used to obtain the cohesion

$$d = \frac{\sigma_z^f \sigma_r^f (\sqrt{13} - 2)}{\sigma_z^f - 2\sigma_r^f} \tag{5}$$

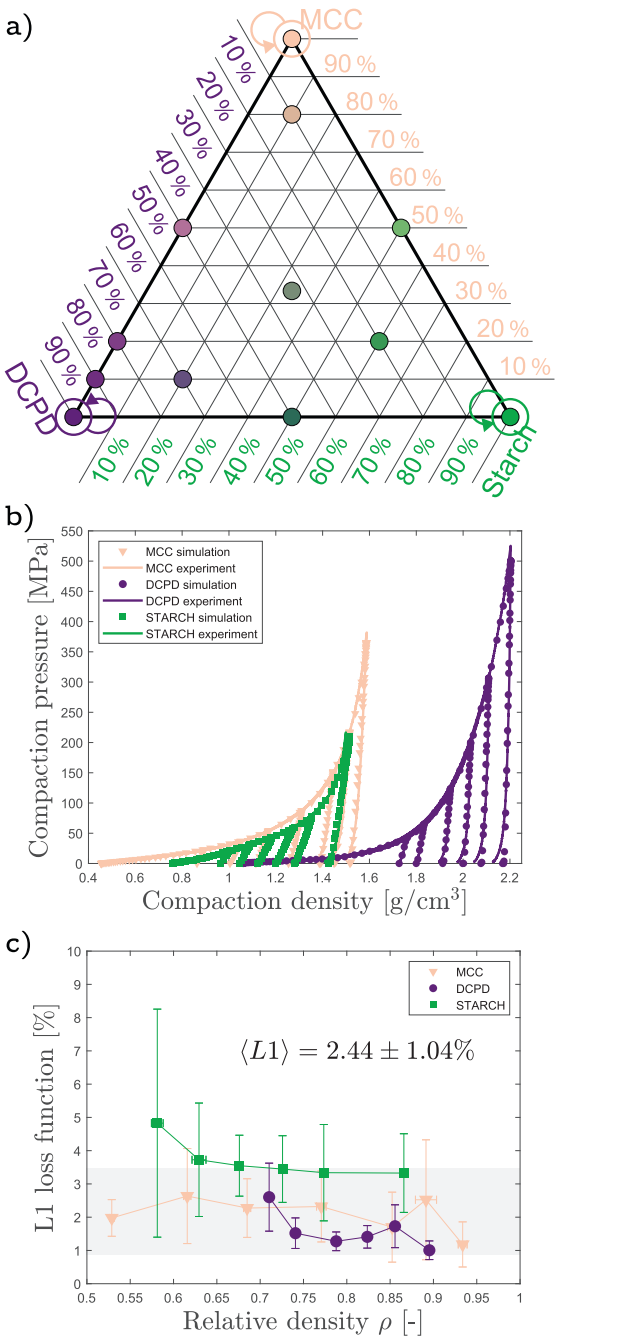

Fig. 1. Compaction simulations with parameters obtained from experimental data accurately reproduce experiment. a) Ternary phase diagram with arrows indicating the parametrisation direction. b) Simulated and experimental compaction curves. c) Average L1 error, with standard deviation, of the simulated compaction curves with respect to experiment. The inset shows the L1 for all displayed data. The grey band shows the average experimental variability plus and minus one standard deviation.

and internal friction angle

$$\beta = \tan^{-1}\left(\frac{3(\sigma_z^f + d)}{\sigma_z^f}\right). \tag{6}$$

Coefficients of friction for the powder-die interaction were determined using

$$\mu = \frac{D}{4zK} \ln\left(\frac{\sigma_T K}{\sigma_r}\right), \tag{7}$$

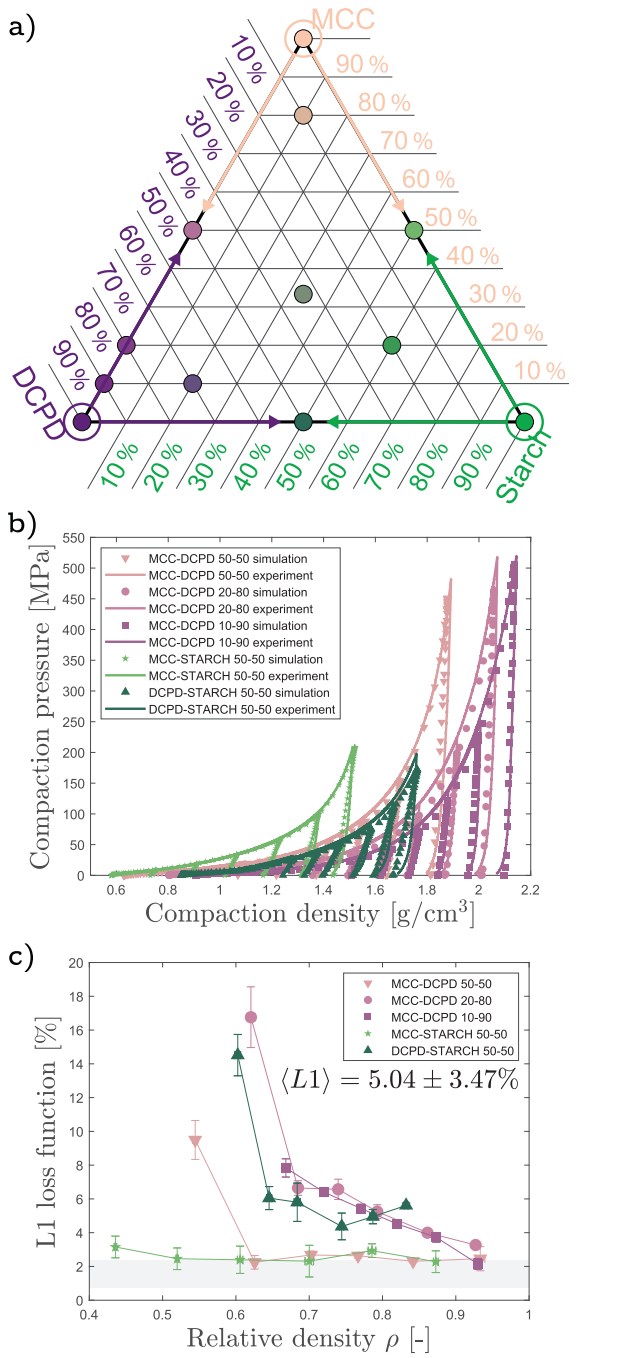

Fig. 2. Binary mixing gives parameters resulting in accurate compaction simulations with respect to experiment. (a) Ternary phase diagram with arrows indicating the parametrisation direction. (b) Simulated and experimental compaction curves. (c) Average L1 error, with standard deviation, of the simulated compaction curves with respect to experiment. The inset shows the L1 for all displayed data. The grey band shows the average experimental variability plus and minus one standard deviation.

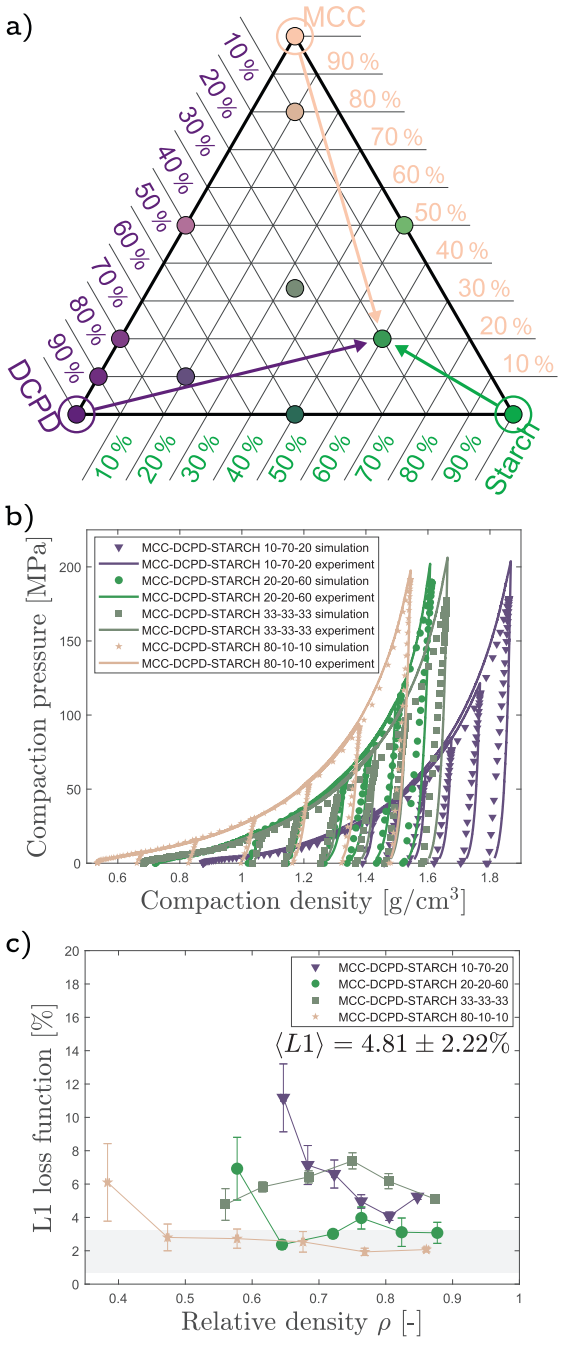

Fig. 3. Ternary mixing gives parameters resulting in accurate compaction simulations with respect to experiment. (a) Ternary phase diagram with arrows indicating the parametrisation direction. (b) Simulated and experimental compaction curves. (c) Average L1 error, with standard deviation, of the simulated compaction curves with respect to experiment. The inset shows the L1 for all displayed data. The grey band shows the average experimental variability plus and minus one standard deviation.

with z the distance between the radial die-wall pressure sensor and the top punch, σ_T the pressure on the top punch, σ_r the radial pressure, and

$$K = \frac{1 + \sin(\beta(\rho))}{1 - \sin(\beta(\rho))}. \tag{8}$$

with β the internal friction angle as given by Eq. 6 [10]. The resulting friction values were between 0.162 and 0.207 with no apparent dependence on the radial pressure.

The effective in-die true density ρ_t of each formulation was determined through a series of high-pressure powder compressions as described in Sun [38,39]. The experimental data of MCC, DCPD, and MCC-DCPD mixtures were previously obtained and used in van der Haven et al. [10].

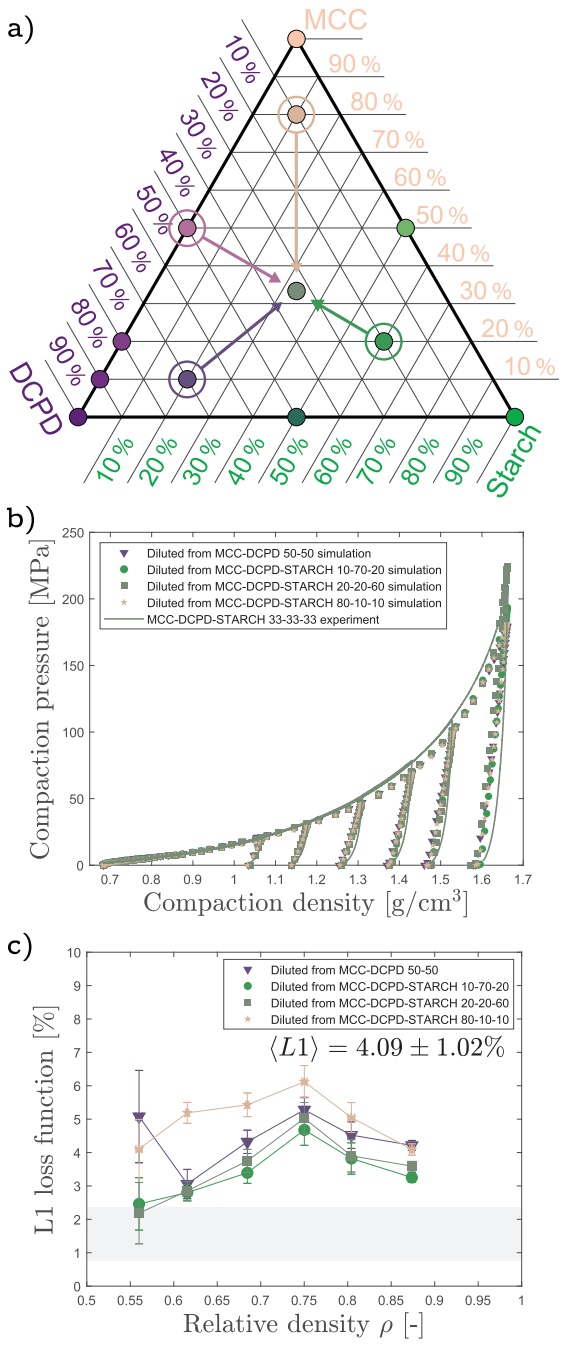

Fig. 4. Dilution by mixing gives parameters resulting in accurate compaction simulations with respect to experiment. (a) Ternary phase diagram with arrows indicating the parametrisation direction. (b) Simulated and experimental compaction curves. (c) Average L1 error, with standard deviation, of the simulated compaction curves with respect to experiment. The inset shows the L1 for all displayed data. The grey band shows the average experimental variability plus and minus one standard deviation.

3. Numerical methods

3.1. Constitutive model

An elasto-plastic model is used to describe the mechanical behaviour of the powder. A popular choice, also used here, is the density-dependent Drucker-Prager Cap (dDPC) model [4,40]. The elastic behaviour is linear and described by the Young's modulus E and Poisson's ratio ν. Plastic deformation can also be described by the dDPC model and said to occur when the stress state of the material crosses the failure surface, which is defined by three segments. The shear failure segment for dilation is given by

$$F_s(p,q) = q - p\tan(\beta) - d = 0. \tag{9}$$

The cap for consolidation is given by

$$F_c(p,q) = \sqrt{(p-p_a)^2 + \left(\frac{Rq}{1+\alpha-\alpha/\cos\beta}\right)^2} - R(d + p_a\tan\beta) = 0 \tag{10}$$

with

$$p_a = \frac{p_b - Rd}{1 + R\tan\beta} \tag{11}$$

where α is a smoothing parameter, R the cap eccentricity, and p_b the compressive hydrostatic yield stress. The transition segment, used to join the previous two segments together, is given by

$$\begin{aligned} F_t(p,q) = &\sqrt{(p-p_a)^2 + \left[q - \left(1 - \frac{\alpha}{\cos\beta}\right)(d + p_a\tan\beta)\right]^2} \\ &- \alpha(d + p_a\tan\beta) \\ &= 0. \end{aligned} \tag{12}$$

Since the mechanical properties of the powders strongly depend on the density, all elastic and plastic parameters are made to be functions of the relative density

$$\rho = \rho_0 \exp(\varepsilon_v^{pl}) \tag{13}$$

where ρ_0 is the relative density of the uncompressed powder in the die and ε_v^{pl} is the volumetric plastic true strain (with compression being positive) [4,41,42].

3.2. Parametrisation

The elastic parameters follow from the first part of the unloading path, from $\max(\sigma_z)$ to $q = 0$ [5,40,41,43]. The Young's modulus is given by

$$E = \frac{(1+\nu)(1-2\nu)}{(1-\nu)}\left(\frac{d\sigma_z}{d\varepsilon_z}\right) \tag{14}$$

with ε_z the axial true strain. The Poisson's ratio is given by

$$\nu = \frac{\left(\frac{d\sigma_r}{d\sigma_z}\right)}{1 + \left(\frac{d\sigma_r}{d\sigma_z}\right)}. \tag{15}$$

Plastic parameters are parametrised as follows. Point A is the point at which σ_z is the highest and is located on the cap yield segment. The cap eccentricity is then

$$R = \sqrt{\frac{2}{3q_A}(1+\alpha-\alpha/\cos\beta)^2(p_A - p_a)}. \tag{16}$$

with

$$p_a = -\frac{3q_A + 4d(1+\alpha-\alpha/\cos\beta)^2\tan\beta}{4[(1+\alpha-\alpha/\cos\beta)\tan\beta]^2} + \frac{\sqrt{9q_A^2 + 24q_A d(1+\alpha-\alpha/\cos\beta)^2\tan\beta + 8\left(3p_A q_A + 2q_A^2\right)[(1+\alpha-\alpha/\cos\beta)\tan\beta]^2}}{4[(1+\alpha-\alpha/\cos\beta)\tan\beta]^2}$$

and the hydrostatic yield stress is

$$p_b = p_a(1 + R\tan\beta) + Rd. \tag{17}$$

The values of d and β follow from Eq. 5 and 6, respectively, and α is set to 0.03. The in-die relative density of the tablet is determined by

taking the density and stress at point A and subtracting the elastic component according to

$$\rho = \frac{\rho_{\mathrm{m,A}}}{\rho_{\mathrm{t}}} \exp\left(-\frac{(1+\nu)(1-2\nu)}{(1-\nu)}\frac{\sigma_{\mathrm{z,A}}}{E}\right). \tag{18}$$

3.3. Mixing rules

Mixing rules can enable predictive FEM simulations of materials for which there are no experimental data [10]. The two core premises of the mixing rules are that 1) the stress on all components is the same and 2) that the properties of the mixture depend on the volume fraction y_i of each component i. A model parameter ξ of a mixture as function of the compaction pressure σ can then be estimated by

$$\xi(\sigma) = \sum_i y_i(\sigma)\xi_i(\sigma), \tag{19}$$

except for the Young's modulus, for which

$$E(\sigma) = \left(\sum_i \frac{y_i(\sigma)}{E_i(\sigma)}\right)^{-1}. \tag{20}$$

This requires the volume fraction of each individual component

$$y_i(\sigma) = y_{0,i}\exp\left(-\varepsilon_{\mathrm{v},i}^{\mathrm{tot}}(\sigma)\right)\left(\sum_j y_{0,j}\exp\left(-\varepsilon_{\mathrm{v},j}^{\mathrm{tot}}(\sigma)\right)\right)^{-1}, \tag{21}$$

which depends on the total volumetric true strain

$$\varepsilon_{\mathrm{v},i}^{\mathrm{tot}}(\sigma) = \int_0^{\sigma}\frac{(1+\nu)(1-2\nu)}{(1-\nu)E_i(\sigma)}\mathrm{d}\sigma + \ln\left(\frac{\rho_i(\sigma)}{\rho_{0,i}}\right). \tag{22}$$

Estimates for the initial volume fractions $y_{0,i}$ are obtained as described in Reynolds et al. [17]. The parameters ξ of the mixture have so far only been described as a function of the stress. However, the numerical implementation of the dDPC model requires all parameters to be a function of the relative density. For the mixture, the relative density is estimated using [16,38]

$$\rho(\sigma) = \left(\sum_i \frac{w_i}{\rho_{\mathrm{t},i}}\right)\sum_i y_i(\sigma)\rho_i(\sigma)\rho_{\mathrm{t},i}. \tag{23}$$

The function $\rho_i(\sigma)$ can be obtained by fitting the compaction density $\rho_{\mathrm{m},i}(\sigma_{\mathrm{z}})$ to the loading curve and then substituting $\rho_{\mathrm{m},i}(\sigma_{\mathrm{z}})$ into another fitted function $\rho_i(\rho_{\mathrm{m}})$ that relates the in-die compaction density to the out-of-die relative density. Previously determined model parameters $\xi_i(\rho_i)$, which are a function of the relative density, can then easily be expressed as a function of σ by substitution of $\rho_i(\sigma)$. Finally, a set of σ values can be generated to obtain a full parameter set $\{\xi(\rho(\sigma)), \rho(\sigma)\}$ for the mixture.

3.4. Demixing rules

Predicting the properties of the individual components within a mixture requires the mixing procedure to be inverted or reversed. To keep the problem tractable, it is assumed that only a single component in a multicomponent mixture is changed, with the ratios between all other components remaining constant. The component of interest will be labelled as component 2 whereas the combination of all other components will be labelled as (composite) component 1. The absence of a subscript denotes a property relating to a complete mixture.

First, the effective true densities need to be estimated. This can be done by least-squares fitting of the linear system

$$\frac{1}{\vec{\rho}_{\mathrm{t}}} = \frac{\vec{w}_1}{\rho_{\mathrm{t},1}} + \frac{(1-\vec{w}_1)}{\rho_{\mathrm{t},2}} \tag{24}$$

with $\vec{\rho}_{\mathrm{t}}$ all the true densities of the known mixtures and $\vec{w}_1$ the associated weight fractions of component 1. The effective true densities $\rho_{\mathrm{t},1}$ and $\rho_{\mathrm{t},2}$ of the components are then determined by the result of the fitting procedure.

The next task is to determine the total volumetric true strains $\varepsilon_{\mathrm{v}}^{\mathrm{tot}}(\sigma)$ of the components by solving the linear system

$$\exp\left(\vec{\varepsilon}_{\mathrm{v}}^{\mathrm{tot}}(\sigma)\right) = \vec{y}_{0,1}\exp\left(\varepsilon_{\mathrm{v},1}^{\mathrm{tot}}(\sigma)\right) + (1-\vec{y}_{0,1})\exp\left(\varepsilon_{\mathrm{v},2}^{\mathrm{tot}}(\sigma)\right) \tag{25}$$

with the estimates for the y_0 values being obtained the same way as in the mixing method [10]. This system is solved for many discrete values of σ, which are then fitted to a B-spline, forced through the point $(0,0)$, to give the continuous functions $\varepsilon_{\mathrm{v},1}^{\mathrm{tot}}(\sigma)$ and $\varepsilon_{\mathrm{v},2}^{\mathrm{tot}}(\sigma)$. Eq. 21 is then used as usual to obtain the volume fractions $y_1(\sigma)$.

The true densities of the mixtures $\vec{\rho}_{\mathrm{t}}$ are determined as in mixing procedure. Then, to determine the relative densities of components 1 and 2 as a function of stress, Eq. 29 from van der Haven et al. is rearranged, with $y_{0,i} = 1$ (being the volume fraction of the complete mixture itself) [10]. This results in a linear system,

$$\frac{1}{\vec{\rho}(\sigma)\vec{\rho}_{\mathrm{t}}} = \frac{\vec{w}_1}{\rho_1(\sigma)\rho_{\mathrm{t},1}} + \frac{(1-\vec{w}_1)}{\rho_2(\sigma)\rho_{\mathrm{t},2}}, \tag{26}$$

which is again solved for many values of σ and fit to a B-spline that is forced through the points $(\rho(0)_1, 0)$ and $(\rho(0)_2, 0)$, respectively, to get $\rho_1(\sigma)$ and $\rho_2(\sigma)$. The functions are forced to be monotonically increasing to assure physicality. The initial compaction density $\rho_{\mathrm{m},2}(0)$ is used to determine $\rho_2(0)$ whereas $\rho_1(0)$ is determined by the fit with $\sigma = 0$ and $\rho_2(0)$.

A range of σ values is generated for the computation of the table of dDPC model parameters that is required for the numerical implementation of the FEM simulations. The relative density follows directly from $\rho_2(\sigma)$. The model parameters $\xi_2(\rho_2(\sigma))$ follow from solving the linear systems given by the mixing rules. Omitting $(\rho(\sigma))$ for brevity, the arithmetic mean gives

$$\vec{\xi} = \vec{y}_1\xi_1 + (1-\vec{y}_1)\xi_2, \tag{27}$$

the geometric mean gives

$$\ln\left(\vec{\xi}\right) = \vec{y}_1\ln(\xi_1) + (1-\vec{y}_1)\ln(\xi_2), \tag{28}$$

and the harmonic mean gives

$$\frac{1}{\vec{\xi}} = \frac{\vec{y}_1}{\xi_1} + \frac{(1-\vec{y}_1)}{\xi_2}, \tag{29}$$

where all of the demixed dDPC parameters are determined using the same mixing rule as in the mixing procedure. An exception is the cohesion d, which uses the geometric mean in the demixing procedure to avoid non-physical negative values.

The demixing procedure also ends up deximing values that are extrapolations of the parametrisations on experimental data. This can lead to some instabilities and requires a correction of the demixed values for E and p_b that are demixed from extrapolated dDPC parameters. On the lower end, both are extrapolated using a quadratic curve starting at $\rho_2(0)$ and ending at the first value of ρ_2 which has not been demixed using extrapolated data. The extrapolations start at 0.1 GPa and 1.0 MPa for E and p_b, respectively. The extrapolation from the experimentally supported values of E to higher values is performed the same way as in van der Haven et al. [10]. For p_b, the extrapolation to high values is done by fitting $c_1\exp(-c_2(c_3-\rho)) + c_4$ to the experimentally supported p_b values of the highest 0.05-wide window of ρ. Finally, the tabulated values of d, R, and p_b are forced to be monotonically increasing. To solve the linear systems in the demixing procedure, only two mixtures are needed but more can be used to improve the accuracy.

3.5. Implementation

All FEM simulations were carried out using Abaqus 2019 by Simulia [44], following the same set up as van der Haven et al. [10]. The built-in DPC model was used and supplemented with a USDFIELD subroutine to add density dependence. Geometric and process parameters of the numerical model were set to be identical to those in experiment. A small taper was added to the die wall to improve numerical stability. The powder and punches were given a regular mesh, while the die wall was given an irregular mesh, with all representations being axisymmetric and deformable. All tooling was given the properties of steel ($E = 210\,\mathrm{GPa}, \nu = 0.3$, and density $7900\,\mathrm{kg\,m^{-3}}$) and 1 mm thick [45]. Outer surfaces of the tooling were constrained with displacement-controlled boundary conditions.

3.6. Error quantification

The L1 loss function is used to quantify the deviation between a given compaction curve and a reference curve, denoted with superscript "ref". The L1 can be expressed either as a fraction or a percentage and is defined as

$$\mathrm{L1} = \left(\int_{\rho^{\mathrm{ref}}_{\mathrm{start}}}^{\rho^{\mathrm{ref}}_{\mathrm{end}}} |\sigma_z - \sigma_z^{\mathrm{ref}}| |\mathrm{d}\rho_m| \right) \times \left(\max\left(\sigma_z^{\mathrm{ref}}\right) \times \int_{\rho^{\mathrm{ref}}_{\mathrm{start}}}^{\rho^{\mathrm{ref}}_{\mathrm{end}}} |\mathrm{d}\rho_m| \right)^{-1}. \tag{30}$$

Physically, the L1 corresponds to the average normalized error per line segment.

4. Results and discussion

4.1. Parametrisation from experimental data

Since the introduction of new powders makes it appropriate to repeat the validation of the parametrisation procedure, we here confirm that the dDPC parametrisation using experimental data as input results in accurate FEM simulations. An automated parametrisation procedure was applied to the newly acquired experimental data to obtain dDPC model parameters, which were then directly used to do FEM simulations. To quantify the error of the simulations with respect to the experiments, we computed the L1 loss function between the simulated and experimental compaction curves. Since each compaction experiment was repeated 10 to 12 times, average L1 loss function are computed, denoted as $\langle \mathrm{L1} \rangle$.

The simulations confirm that, aside from MCC (plastic) and DCPD (brittle), the compaction behaviour of the starch (elastic) can also be reproduced (Fig. 1). The reader is referred to the supplementary for figures of the simulations for the mixtures (Fig. S4–S7). For all 12 formulations, making a total of 73 unique tablets, this resulted in an error of $\langle \mathrm{L1} \rangle = 2.93 \pm 1.70\%$. To get a better feel for the magnitude of the L1 values, we also computed the experimental variability, i.e. the average L1 between all pairs of replicate experiments. This gives an experimental variability of $\langle \mathrm{L1} \rangle = 1.85 \pm 1.12\%$ over all experiments. The simulation error is thus only marginally higher than the experimental variability, showing that the parametrisation procedure results in highly accurate and precise FEM simulations for a broad range of powders with drastically different mechanical properties.

4.2. Multi-component mixing

We now continue to demonstrate that the mixing methodology can be used to perform FEM simulations of powder mixtures when only experimental data for their pure constituent powders is available. Thus, only the experimental data of pure MCC, DCPD, and starch are used as input for the simulations here. Following up on van der Haven et al. [10], the mixing methodology was tested on two new binary mixtures, MCC-starch and DCPD-starch (Fig. 2). The average L1 value is around 5%, thereby remaining similar to that previously reported for binary mixture prediction. Moreover, the mixing methodology was tested on four ternary mixtures (Fig. 3). The accuracy of the predictions for ternary mixtures appears to be similar to that for binary mixtures, demonstrating

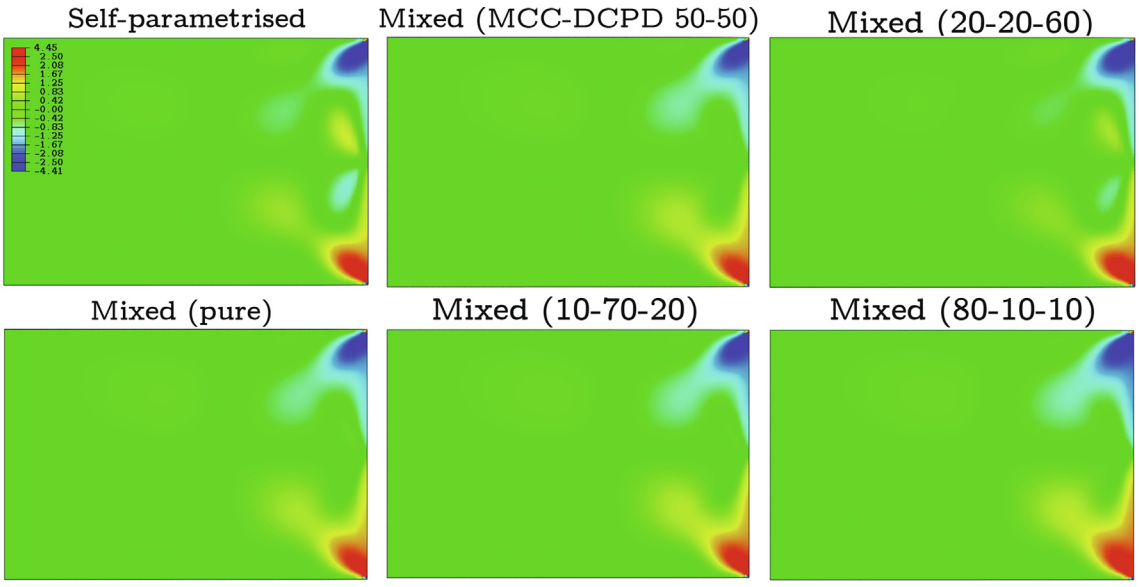

Fig. 5. Profiles of the shear stress in MPa of the second-to–highest density tablet of MCC-DCPD-starch (with 33% of each component) after unloading, resulting from different methodologies. The similarity of the profiles shows that the mixing methodology works regardless of the chosen starting material or input data. Because of radial symmetry, only half the tablet's vertical cross-section is shown here, with the left edge being the centre axis and the right edge being the side touching the die wall. "Self-parametrised" means that model parameters followed directly from experimental data. "Mixed" means that model parameters followed from the mixing methodology with the starting mixture between brackets (weight percentages of MCC-DCPD-starch) as shown in Fig. 3 and 4.

that the mixing methodology is valid and accurate for binary as well as multi-component mixtures. Overall, mixtures were predicted with $\langle L1 \rangle = 4.94 \pm 2.95\%$.

Similar to previous work [10], a higher error is generally observed for predictions for the lowest tablet density (Fig. 2c). Because the parametrisation starts at the final density of the most porous tablet, these simulations mainly rely on extrapolated parameters, increasing the error. This error is likely further aggravated when applying the mixing rules. However, the function of the lowest-density data is much more to support the stability of the method than to be a potential target within the formulation design space. Tablets at the lowest reported density barely form cohesive tablets and would be unsuitable for any practical application because their tensile strength would be too low to meet the required industry standards [31,32]. The increased error at the lowest density therefore does not diminish the usefulness of the presented methods. Instead, the presence of the lowest-density data points means that less parameter extrapolation is necessary,

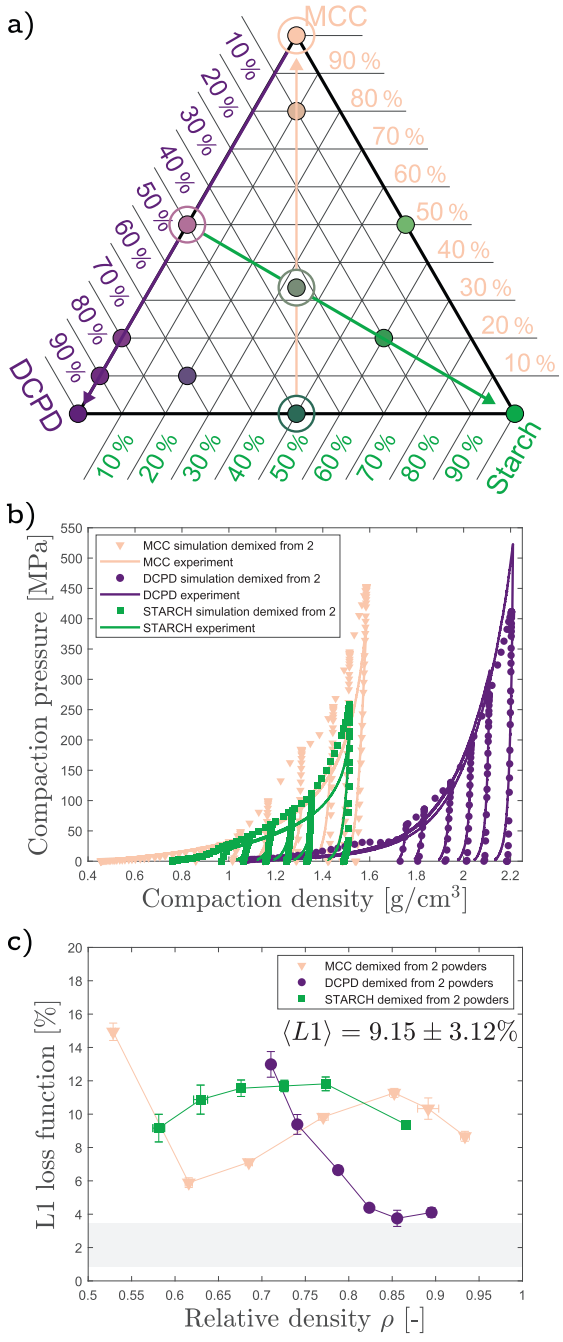

Fig. 6. Demixing using two experimental formulations as input gives parameters resulting in reasonably accurate compaction simulations with respect to experiment. (a) Ternary phase diagram with arrows indicating the parametrisation direction. (b) Simulated and experimental compaction curves. (c) Average L1 error, with standard deviation, of the simulated compaction curves with respect to experiment. The inset shows the L1 for all displayed data. The grey band shows the average experimental variability plus and minus one standard deviation.

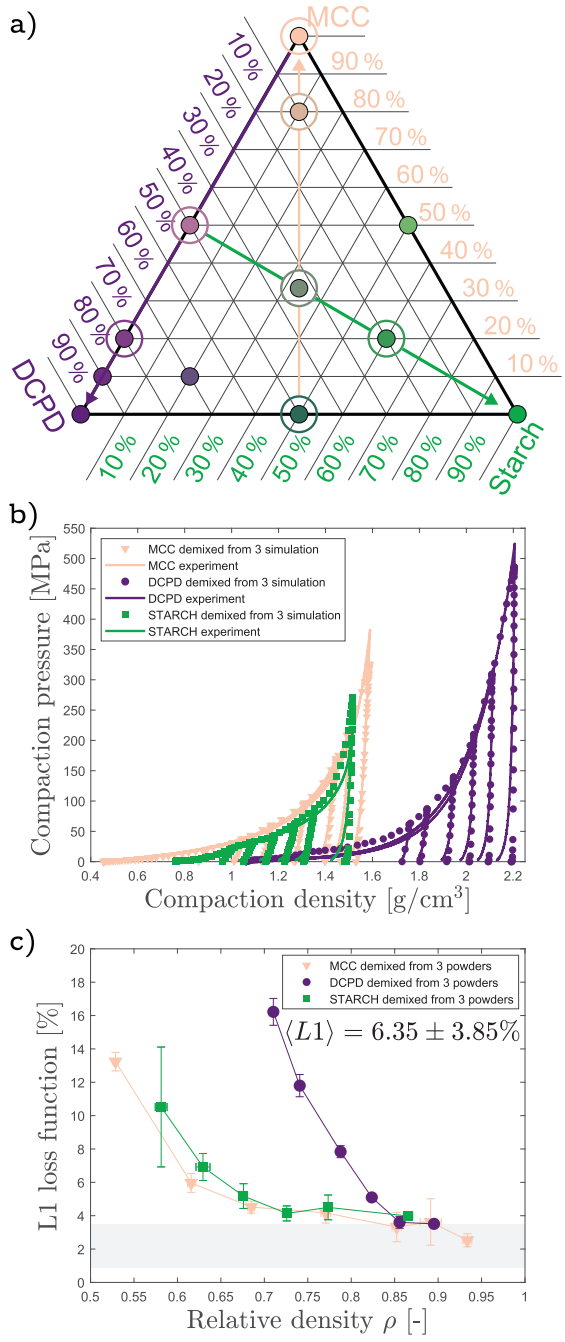

Fig. 7. Demixing using three experimental formulations as input gives parameters resulting in accurate compaction simulations with respect to experiment. (a) Ternary phase diagram with arrows indicating the parametrisation direction. (b) Simulated and experimental compaction curves. c) Average L1 error, with standard deviation, of the simulated compaction curves with respect to experiment. The inset shows the L1 for all displayed data. The grey band shows the average experimental variability plus and minus one standard deviation.

improving the stability and accuracy of simulations at densities that do fall within the viable formulation design space.

To put the performance of the mixing methodology into further context, we should consider the types of materials used and whether they are applicable to industrially relevant problems. MCC is generally considered to be plastic, DCPD is considered brittle, and starch is considered (visco-)elastic. MCC and starch can therefore be said to behave more like typical excipients, whereas DCPD behaves more like a typical crystalline active pharmaceutical ingredient (API). The mechanical properties of the constituent powders are thus varied greatly, showing that the mixing methodology is robust and applicable to realistic powder formulations used in the pharmaceutical industry.

4.3. Dilution

So far, the application of the mixing methodology has been limited to using only input parameters of the pure constituent powders, despite the common knowledge that not all pure powders can be compacted into intact tablets, as required to obtain model parameters. This limitation is addressed here by showing that parameters of powder mixtures themselves can also be used as input. Mixtures can be diluted into other formulations by mixing them with only a small number of pure components. For example, Fig. 4 shows that, regardless of the initial mixture, dilution produces accurate predictions for the central mixture with equal parts of MCC, DCPD, and starch. Fig. 5 further shows that the resulting shear-stress profiles at the end of unloading are also nearly identical.

The errors resulting from dilution are even lower than those resulting from mixing, presumably because of the shorter distance between the input data and the target formulation. There is also no reason to suspect that mixtures themselves cannot be combined. Being able to combine mixtures as well as pure-component powders greatly extends the capabilities of the mixing methodology. However, in spite of this added flexibility, the domain of possible predictions is still limited to a certain region of the phase diagram. This region is marked by the convex hull of all tested or known compositions in the phase diagram. Dilution will thus always require, for each individual component, experimental data of a formulation that has a higher fraction of that component.

4.4. Demixing

To fully lift the limitations on the powder compositions that can be predicted, a demixing or extrapolation methodology is needed, which is demonstrated here using the demixing methodology proposed earlier. Using the absolute minimum of two input formulations, Fig. 6 shows the predicted compaction curves for the demixed pure components. Given that the input formulations only contain 33% to 50% of the target material at most, the performance is surprisingly good.

However, not all combinations lead to accurate predictions. For example, using the MCC-starch and central MCC-DCPD-starch mixture to predict pure DCPD does not seem to work as the predicted Young's moduli become negative. The parameter extrapolations naturally become less reliable as the distance from the experimental input data increases. It is also unsurprising that DCPD requires higher weight fractions for reliable prediction, because it is also the most mechanically unique powder. Moreover, using only two formulations for the input means that any error is immediately propagated. This is not the case when three or more formulations are used, as the regression in the demixing methodology distributes the error. Fig. 7 shows that using one extra formulation to do

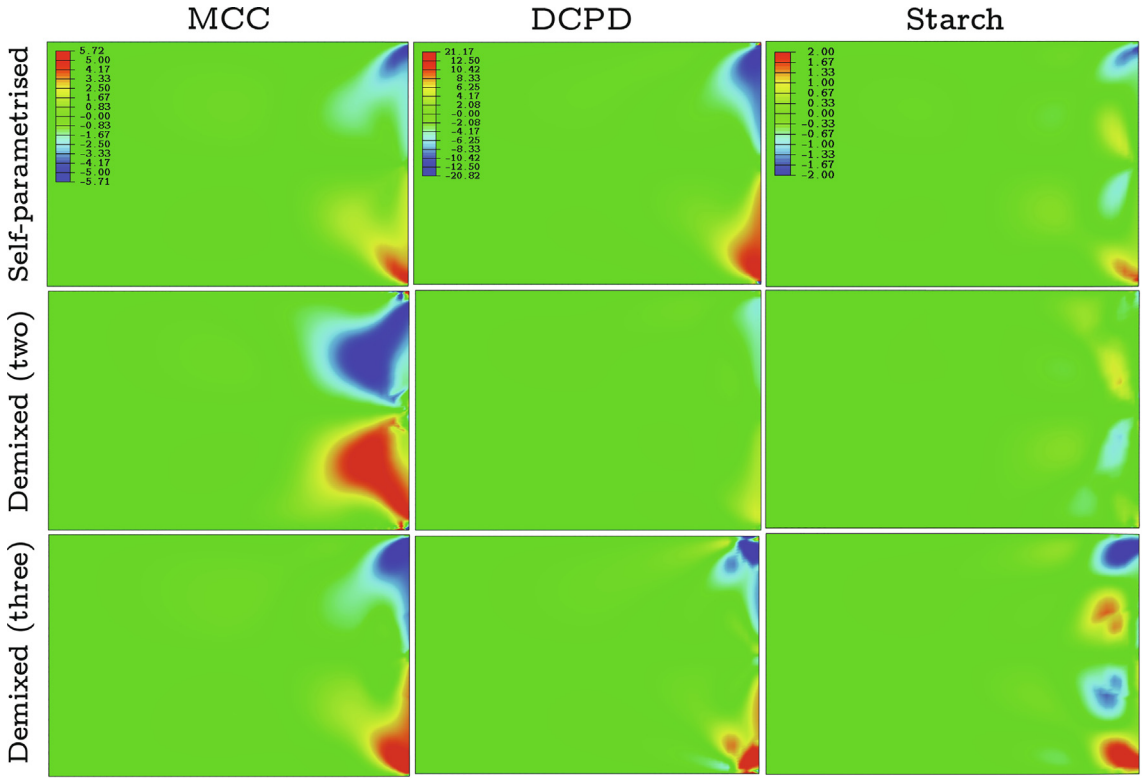

Fig. 8. The shear stress profiles in MPa within the vertical cross-section of the second-to–highest density tablet after unloading, demonstrating that the demixing methodology produces the same qualitative trends. The columns indicate the material whereas the row indicates how the model parameters were obtained. "Self-parametrised" means that model parameters followed directly from experimental data. "Demixed" means parameters were obtained from the demixing methodology using either two or three input formulations as given in Fig. 6 and 7. Similar to Fig. 5, only half of the vertical cross-section is shown..

pure-component predictions results in more accurate predictions, only about a single percentage point less accurate than the mixing rules. Given that API properties can change significantly as part of the normal API development, this level of accuracy incredibly useful for early formulation selection.

But most of all, compared to directly parametrised simulations, Fig. 8 shows that the demixing methodology results in similar shear stress profiles at the end of unloading, both qualitatively and quantitatively. MCC and DCPD show higher shear regions near the top and bottom edges of the tablet, whereas starch shows a more alternating shear pattern. The demixing methodology therefore provides a novel way of compaction curves and stress profiles for poorly tabletable, or otherwise untested, powder formulations.

Partial demixing is of course also possible, even expected to be more accurate, by artificially adjusting the weight fractions at the start of the demixing procedure such that $w_2 = 1$ gives the desired mixture. The restriction of only being able to demix in a straight line across the phase diagram can be lifted by combining the mixing and demixing methodologies. The reported methodologies thereby enable us to reach the full phase diagram, regardless of whether the individual components are tabletable or not. Strictly speaking, by repeating the mixing and demixing procedures, one would only need to test N distinct formulations of a powder containing N unique components to estimate the whole N-dimensional phase diagram. The testing of any additional formulations would only serve to reduce the error of the predictions. Many of the formulations discussed in the current work can thus be predicted using more than one of the three strategies, being mixing, dilution, and demixing. In general, the recommendation is to use the approach that minimises the distance between the target mixture and the known mixtures since this results in the lowest error.

5. Conclusions

The current work greatly extends the validation of the automated dDPC model parametrisation procedure reported previously. FEM simulations using dDPC parameters derived directly from experimental data reproduced experimental compaction curves with an average L1 loss function of $\langle L1 \rangle = 2.93 \pm 1.7\%$ of the maximum compaction pressure, a good performance compared to the experimental variability of $\langle L1 \rangle = 1.85 \pm 1.12\%$. The mixing methodology, by combining dDPC model parameters of the pure constituent powders, was able to predict experimental compaction curves of binary and ternary mixtures with $\langle L1 \rangle = 4.94 \pm 2.95\%$. Similarly, the mixing methodology could be applied to mixtures, effectively diluting the formulation, giving $\langle L1 \rangle = 4.09 \pm 1.02\%$. Shear stress profiles resulting from the FEM simulations were furthermore nearly identical, regardless of how the model parameters were obtained.

Moreover, a novel demixing methodology was developed to estimate the dDPC model parameters of formulations that lie outside the domain of tested formulations, effectively allowing predictions of even non-tabletable powders or formulations. Depending on whether experimental data of two or three formulations was used, FEM simulations of pure powders using demixed parameters resulted in modest errors of $\langle L1 \rangle = 9.15 \pm 3.12\%$ and $\langle L1 \rangle = 6.35 \pm 3.85\%$, respectively. Shear stress profiles were both qualitatively and quantitatively similar, further supporting the validity of the new mixing methodology.

Together, these developments allow exploration of the full phase diagram of powder formulations, needing only minimal experimental input data. Compaction curves and stress profiles of any mixture can thus be predicted, providing a level of detail unattainable by conventional mixing methods or rules. These new methodologies can become indispensable tools for process development in pharmaceutical powder compaction, providing information that is critical for the consideration of joint formulation and punch-design optimisation.

Declaration of Competing Interest

The authors declare that they have no known competing financial interests or personal relationships that could have appeared to influence the work reported in this paper.

Acknowledgements

This project has been financed by Novo Nordisk A/S (Bagsværd, Denmark).

Appendix A. Supplementary material

Supplementary data associated with this article can be found, in the online version, at https://doi.org/10.1016/j.apt.2024.104513.

References

[1] P.G. de Gennes, Granular matter: a tentative view, Rev. Mod. Phys. 71 (2) (1999) S374–S382. https://doi.org/10.1103/RevModPhys.71.S374.
[2] Q. Sun, G. Wang, K. Hu, Some open problems in granular matter mechanics, Prog. Nat. Sci. 19 (5) (2009) 523–529. https://doi.org/10.1016/j.pnsc.2008.06.023.
[3] A. Baule, F. Morone, H.J. Herrmann, H.A. Makse, Edwards statistical mechanics for jammed granular matter, Rev. Mod. Phys. 90 (1) (2018) 015006. https://doi.org/10.1103/RevModPhys.90.015006.
[4] I. Sinka, J. Cunningham, A. Zavaliangos, The effect of wall friction in the compaction of pharmaceutical tablets with curved faces: a validation study of the drucker–prager cap model, Powder Technol. 133 (1–3) (2003) 33–43.
[5] A. Krok, M. Peciar, R. Fekete, Numerical investigation into the influence of the punch shape on the mechanical behavior of pharmaceutical powders during compaction, Particuology 16 (2014) 116–131. https://doi.org/10.1016/j.partic.2013.12.003.
[6] H. Diarra, V. Mazel, V. Busignies, P. Tchoreloff, Sensitivity of elastic parameters during the numerical simulation of pharmaceutical die compaction process with Drucker-Prager/Cap model, Powder Technol. 332 (2018) 150–157. https://doi.org/10.1016/j.powtec.2018.03.068.
[7] H. Diarra, V. Mazel, V. Busignies, P. Tchoreloff, FEM simulation of the die compaction of pharmaceutical products: Influence of visco-elastic phenomena and comparison with experiments, Int. J. Pharm. 453 (2) (2013) 389–394. https://doi.org/10.1016/j.ijpharm.2013.05.038.
[8] A. Krok, N. Vitorino, J. Zhang, J.R. Frade, C.-Y. Wu, Thermal properties of compacted pharmaceutical excipients, Int. J. Pharm. 534 (1) (2017) 119–127. https://doi.org/10.1016/j.ijpharm.2017.10.018.
[9] I. Partheniadis, V. Terzi, I. Nikolakakis, Finite Element Analysis and Modeling in Pharmaceutical Tableting, Pharmaceutics 14 (3) (2022) 673. https://doi.org/10.3390/pharmaceutics14030673.
[10] D.L.H. van der Haven, F.H. Ørtoft, K. Naelapää, I.S. Fragkopoulos, J.A. Elliott, Predictive modelling of powder compaction for binary mixtures using the finite element method, Powder Technol. 403 (2022) 117381. https://doi.org/10.1016/j.powtec.2022.117381.
[11] V. Busignies, B. Leclerc, P. Porion, P. Evesque, G. Couarraze, P. Tchoreloff, Investigation and modelling approach of the mechanical properties of compacts made with binary mixtures of pharmaceutical excipients, Eur. J. Pharm. Biopharm. 64 (1) (2006) 51–65. https://doi.org/10.1016/j.ejpb.2006.03.010.
[12] V. Busignies, P. Evesque, P. Porion, B. Leclerc, P. Tchoreloff, Mechanical properties of compacts made with binary mixtures of pharmaceutical excipients of three different kinds, AIP Conf. Proc. 1145 (1) (2009) 240–243. https://doi.org/10.1063/1.3179902.
[13] G. Bano, Z. Wang, P. Facco, F. Bezzo, M. Barolo, M. Ierapetritou, A novel and systematic approach to identify the design space of pharmaceutical processes, Comput. Chem. Eng. 115 (2018) 309–322. https://doi.org/10.1016/j.compchemeng.2018.04.021.
[14] H.M. Zawbaa, S. Schiano, L. Perez-Gandarillas, C. Grosan, A. Michrafy, C.-Y. Wu, Computational intelligence modelling of pharmaceutical tabletting processes using bio-inspired optimization algorithms, Adv. Powder Technol. 29 (12) (2018) 2966–2977. https://doi.org/10.1016/j.apt.2018.11.008.
[15] C.-Y. Wu, S.M. Best, A.C. Bentham, B.C. Hancock, W. Bonfield, A simple predictive model for the tensile strength of binary tablets, Eur. J. Pharm. Sci. 25 (2) (2005) 331–336. https://doi.org/10.1016/j.ejps.2005.03.004.
[16] C.-Y. Wu, S.M. Best, A.C. Bentham, B.C. Hancock, W. Bonfield, Predicting the Tensile Strength of Compacted Multi-Component Mixtures of Pharmaceutical Powders, Pharm. Res. 23 (8) (2006) 1898–1905. https://doi.org/10.1007/s11095-006-9005-6.

[17] G.K. Reynolds, J.I. Campbell, R.J. Roberts, A compressibility based model for predicting the tensile strength of directly compressed pharmaceutical powder mixtures, Int. J. Pharm. 531 (1) (2017) 215–224. https://doi.org/10.1016/j.ijpharm.2017.08.075.
[18] I. Wünsch, J.H. Finke, E. John, M. Juhnke, A. Kwade, Influence of the drug deformation behaviour on the predictability of compressibility and compactibility of binary mixtures, Int. J. Pharm. 626 (2022) 122117. https://doi.org/10.1016/j.ijpharm.2022.122117.
[19] G. Frenning, J. Nordström, G. Alderborn, Effective Kawakita parameters for binary mixtures, Powder Technol. 189 (2) (2009) 270–275. https://doi.org/10.1016/j.powtec.2008.04.016.
[20] V. Mazel, V. Busignies, S. Duca, B. Leclerc, P. Tchoreloff, Original predictive approach to the compressibility of pharmaceutical powder mixtures based on the Kawakita equation, Int. J. Pharm. 410 (1) (2011) 92–98. https://doi.org/10.1016/j.ijpharm.2011.03.027.
[21] V. Busignies, V. Mazel, H. Diarra, P. Tchoreloff, Prediction of the compressibility of complex mixtures of pharmaceutical powders, Int. J. Pharm. 436 (1) (2012) 862–868. https://doi.org/10.1016/j.ijpharm.2012.06.051.
[22] S. Berkenkemper, S. Klinken, P. Kleinebudde, Investigating compressibility descriptors for binary mixtures of different deformation behavior, Powder Technol. 424 (2023) 118571. https://doi.org/10.1016/j.powtec.2023.118571.
[23] M. Capece, R. Ho, J. Strong, P. Gao, Prediction of powder flow performance using a multi-component granular Bond number, Powder Technol. 286 (2015) 561–571. https://doi.org/10.1016/j.powtec.2015.08.031.
[24] M. Capece, K.R. Silva, D. Sunkara, J. Strong, P. Gao, On the relationship of inter-particle cohesiveness and bulk powder behavior: Flowability of pharmaceutical powders, Int. J. Pharm. 511 (1) (2016) 178–189. https://doi.org/10.1016/j.ijpharm.2016.06.059.
[25] A.L.P. Queiroz, W. Faisal, K. Devine, H. Garvie-Cook, S. Vucen, A.M. Crean, The application of percolation threshold theory to predict compaction behaviour of pharmaceutical powder blends, Powder Technol. 354 (2019) 188–198. https://doi.org/10.1016/j.powtec.2019.05.027.
[26] S. Paul, C. Wang, C.C. Sun, An extended macroindentation method for determining the hardness of poorly compressible materials, Int. J. Pharm. 624 (2022) 122054. https://doi.org/10.1016/j.ijpharm.2022.122054.
[27] H.G. Jolliffe, F. Papathanasiou, E. Prasad, G. Halbert, J. Robertson, C.J. Brown, A.J. Florence, Improving the prediction of multi-component tablet properties from pure component parameters, in: Computer Aided Chemical Engineering, Vol. 46, Elsevier, Walthm, MA, USA, 2019, pp. 883–888. doi:10.1016/B978-0-12-818634-3.50148-X.
[28] H.G. Jolliffe, E. Ojo, C. Mendez, I. Houson, R. Elkes, G. Reynolds, A. Kong, E. Meehan, F.A. Becker, P.M. Piccione, S. Verma, A. Singaraju, G. Halbert, J. Robertson, Linked experimental and modelling approaches for tablet property predictions, Int. J. Pharm. 626 (2022) 122116. https://doi.org/10.1016/j.ijpharm.2022.122116.
[29] D. Puckhaber, J.H. Finke, S. David, M. Serratoni, U. Zafar, E. John, M. Juhnke, A. Kwade, Prediction of the impact of lubrication on tablet compactibility, Int. J. Pharm. 617 (2022) 121557. https://doi.org/10.1016/j.ijpharm.2022.121557.
[30] D. Puckhaber, A.-L. Voges, S. Rane, S. David, B. Gururajan, J.H. Finke, A. Kwade, Enhanced Multi-Component Model to Describe the Lubricant Effect on Compressibility and Compactibility, [Online; accessed 23. Mar. 2023] (Feb. 2023). doi:10.2139/ssrn.4355149.
[31] European Pharmacopoeia (Ph. Eur.) 11th Edition - European Directorate for the Quality of Medicines & HealthCare - EDQM, [Online; accessed 30. Jun. 2023] (Jun. 2023). https://www.edqm.eu/en/european-pharmacopoeia-ph.-eur.-11th-edition#%7B%22468369%22:%5B2%5D%7D.
[32] US Pharmacopeia (USP), Reference Standards, [Online; accessed 30. Jun. 2023] (Jun. 2023). URL https://www.usp.org/reference-standards.
[33] C.-Y. Wu, O.M. Ruddy, A.C. Bentham, B.C. Hancock, S.M. Best, J.A. Elliott, Modelling the mechanical behaviour of pharmaceutical powders during compaction, Powder Technol. 152 (1) (2005) 107–117. https://doi.org/10.1016/j.powtec.2005.01.010.
[34] M.S. Kadiri, A. Michrafy, The effect of punch's shape on die compaction of pharmaceutical powders, Powder Technol. 239 (2013) 467–477. https://doi.org/10.1016/j.powtec.2013.02.022.
[35] V. Mazel, L. Desbois, P. Tchoreloff, Influence of the unloading conditions on capping and lamination: Study on a compaction simulator, Int. J. Pharm. 567 (2019) 118468. https://doi.org/10.1016/j.ijpharm.2019.118468.
[36] J. Meynard, F. Amado-Becker, P. Tchoreloff, V. Mazel, On the complexity of predicting tablet capping, Int. J. Pharm. 623 (2022) 121949. https://doi.org/10.1016/j.ijpharm.2022.121949.
[37] G. Alonso Aruffo, M. Michrafy, D. Oulahna, A. Michrafy, Modelling powder compaction with consideration of a deep grooved punch, Powder Technol. 395 (2022) 681–694. https://doi.org/10.1016/j.powtec.2021.10.012.
[38] C.C. Sun, A novel method for deriving true density of pharmaceutical solids including hydrates and water-containing powders, J. Pharm. Sci. 93 (3) (2003) 646–653. https://doi.org/10.1002/jps.10595.
[39] M. Kuentz, H. Leuenberger, Pressure susceptibility of polymer tablets as a critical property: A modified heckel equation, J. Pharm. Sci. 88 (2) (1999) 174–179. https://doi.org/10.1021/js980369a.
[40] A. Michrafy, D. Ringenbacher, P. Tchoreloff, Modelling the compaction behaviour of powders: application to pharmaceutical powders, Powder Technol. 127 (3) (2002) 257–266.
[41] L. Han, J. Elliott, A. Bentham, A. Mills, G. Amidon, B. Hancock, A modified drucker-prager cap model for die compaction simulation of pharmaceutical powders, Int. J. Solids Struct. 45 (10) (2008) 3088–3106.
[42] T. Sinha, R. Bharadwaj, J.S. Curtis, B.C. Hancock, C. Wassgren, Finite element analysis of pharmaceutical tablet compaction using a density dependent material plasticity model, Powder Technol. 202 (1) (2010) 46–54. https://doi.org/10.1016/j.powtec.2010.04.001.
[43] C.-Y. Wu, O. Ruddy, A. Bentham, B. Hancock, S. Best, J. Elliott, Modelling the mechanical behaviour of pharmaceutical powders during compaction, Powder technology 152 (1–3) (2005) 107–117.
[44] K. Hibbitt, B. Karlsson, P. Sorensen, Abaqus: User's manual: Hibbitt, Karlsson & Sorensen (1988).
[45] H.E. Krex, Maskin ståbi, Teknisk forlag, 1978.